

## ARTICLES

## Carbon Nanotubes from Organometallic Precursors

C. N. R. RAO\* AND A. GOVINDARAJ

*Chemistry and Physics of Materials Unit and CSIR Centre of Excellence in Chemistry, Jawaharlal Nehru Centre for Advanced Scientific Research, Jakkur P. O., Bangalore 560 064, India*

Received January 7, 2002

## ABSTRACT

Multiwalled as well as single-walled carbon nanotubes are conveniently prepared by the pyrolysis of organometallic precursors such as metallocenes and phthalocyanines in a reducing atmosphere. More importantly, pyrolysis of organometallics alone or in mixture with hydrocarbons yields aligned nanotube bundles with useful field emission and hydrogen storage properties. By pyrolysis of organometallics in the presence of thiophene, Y-junction nanotubes are obtained in large quantities. The Y-junction tubes have a good potential in nanoelectronics. Carbon nanotubes prepared from organometallics are useful to prepare nanowires and nanotubes of other materials such as BN, GaN, SiC, and Si<sub>3</sub>N<sub>4</sub>.

## Introduction

Carbon nanotubes were discovered as a microscopic miracle in the cathode deposits obtained in the arc evaporation of graphite.<sup>1</sup> The arc method has since been improved and modified to obtain good yields of both multiwalled and single-walled nanotubes. Carbon nanotubes are conveniently obtained by carrying out the pyrolysis of hydrocarbons such as ethylene and acetylene over nanoparticles of iron, cobalt, and other metals dispersed over a solid substrate.<sup>2–4</sup> The presence of nanoparticles is essential not only to form nanotubes but also to control the diameter of the nanotube to some extent.<sup>5</sup> Since a carbon source as well as metal nanoparticles is necessary for producing carbon nanotubes by the pyrolysis of hydrocarbons, the strategy of employing an appropriate organometallic precursor which can serve as a dual source of both the carbon and the metal nanoparticles was explored by us. The very first experiments carried out on the pyrolysis of organometallic precursors

such as metallocenes and iron pentacarbonyl were successful in producing multiwalled nanotubes.<sup>6,7</sup> We have employed this method not only to produce multiwalled and single-walled nanotubes but also to make aligned nanotube bundles and Y-junction nanotubes. In this Account, we present the salient features of the various types of nanotubes obtained by us in Bangalore by employing the organometallic route and also examine some of the properties of the nanotubes so produced. Aligned nanotube bundles are expected to have applications in electronic displays and hydrogen storage while Y-junction nanotubes could be useful as building blocks in nanoelectronics. The nanotubes produced from organometallics are also usefully employed as starting materials to prepare other types of nanostructures.

## Multiwalled and Single-Walled Nanotubes

Sen et al.<sup>6</sup> prepared multiwalled carbon nanotubes (MWNTs) and metal-filled onionlike structures by the pyrolysis of metallocenes such as ferrocene, cobaltocene, and nickelocene under reducing conditions, wherein the precursor acts as the source of the metal as well as carbon. The pyrolysis setup consists of stainless steel gas flow lines and a two-stage furnace system fitted with a quartz tube (25 mm i.d.) as shown in Figure 1a, the flow rate of the gases being controlled by the use of mass flow controllers. In a typical preparation, a known quantity (100 mg) of the metallocene (presublimed 99.99% purity) is taken in a quartz boat and placed at the center of the first furnace, and a mixture of Ar and H<sub>2</sub> of the desired composition is passed through the quartz tube. The metallocene is sublimed by raising the temperature of the first furnace to 200 °C at a controlled heating rate (20 °C/min). The metallocene vapor so generated is carried by the Ar–H<sub>2</sub> gas stream into the second furnace, maintained at 900 °C, where the pyrolysis occurs. The main variables in the experiment are the heating rate of ferrocene, the flow rate of Ar gas, and the pyrolysis temperature. Ferrocene vapor carried by a 75% Ar + 25% H<sub>2</sub> mixture at a flow rate of 900 sccm (sccm = standard cubic centimeter per minute) into the furnace yields large quantities of carbon deposits, mainly containing carbon nanotubes. These deposits are examined by a scanning electron microscope (SEM) and transmission electron microscope (TEM). In Figure 2a, we show a TEM image of nanotubes produced by the pyrolysis of ferrocene. To increase the yield of the multiwalled carbon nanotubes with metallocene, vapors of an additional hydrocarbon source were mixed along with the metallocene vapor in the first furnace. Thus, pyrolysis of benzene in the presence of ferrocene or Fe(CO)<sub>5</sub> gives high yields of multiwalled nanotubes, the wall thickness of the nanotubes depending on the proportion of the carbon

C. N. R. Rao obtained his Ph.D. degree from Purdue University and D.Sc. degree from the University of Mysore. He is Linus Pauling Research Professor at the JNCASR and Honorary Professor at the Indian Institute of Science, Bangalore, India. He is a member of several academies including the Royal Society (London), U.S. National Academy of Sciences, French Academy of Sciences, and Japan Academy. His main research interests are in solid state and materials chemistry and nanomaterials. The most recent award received by him is the Hughes medal for physical sciences from the Royal Society.

A. Govindaraj obtained his Ph.D. degree from the University of Mysore and is a Scientific Officer at the Indian Institute of Science, Bangalore, India, and Honorary Senior Research Officer at the JNCASR. His main research interests are nanotubes and fullerenes. He is a recipient of the MRS (India) medal.

\* To whom correspondence should be addressed. Fax: 91-80-8462760. E-mail: cnrrao@jncasr.ac.in.

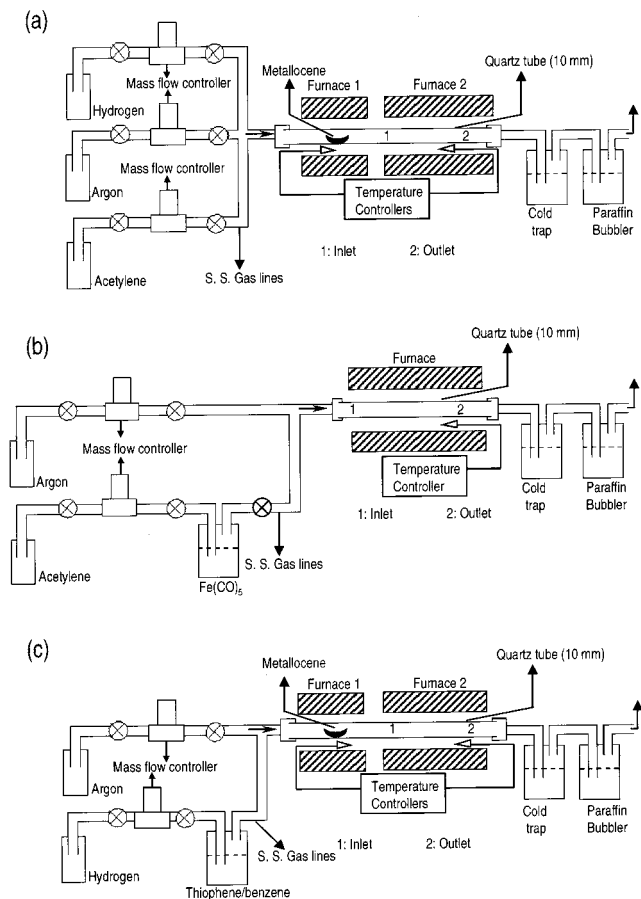


**FIGURE 1.** Pyrolysis apparatus employed for the synthesis of carbon nanotubes by pyrolysis of mixtures of (a) metalocene +  $C_2H_2$ , (b)  $Fe(CO)_5$  +  $C_2H_2$ , and (c) metalocene + benzene or thiophene. The numbers 1 and 2 indicated in the figure represents inlet and outlet, respectively.<sup>6</sup>

source and the metal precursor.<sup>7</sup> In Figure 2b, we show a TEM image of nanotubes obtained by the pyrolysis of a mixture of  $C_2H_2$  (25 sccm) and ferrocene at 1100 °C in a Ar flow rate of 1000 sccm. The image clearly reveals that the addition of hydrocarbon not only increases the yield of hollow MWNTs but also reduces the amount of carbon-coated metal nanoparticles. In Figure 2c we show a TEM image of MWNTs obtained by the pyrolysis of a mixture of nickelocene and benzene at 900 °C in 85% Ar and 15%  $H_2$  mixture at a flow rate of 1000 sccm. Besides metalocenes, one can also employ metal phthalocyanines as precursors to prepare MWNTs.<sup>8,9</sup>

To prepare single-walled nanotubes (SWNTs), alternate synthetic strategies have been explored. Under controlled conditions of pyrolysis, dilute hydrocarbon–organometallic mixtures yield SWNTs.<sup>10,11</sup> High-resolution TEM images of SWNTs, obtained by the pyrolysis of a nickelocene–acetylene mixture at 1100 °C,<sup>11</sup> are shown in the Figure 3a,b. The diameter of the SWNT in Figure 3a is 1.4 nm. It may be recalled that the pyrolysis of nickelocene in admixture with benzene under similar conditions primarily yields MWNTs. Acetylene appears to be a better carbon source for the preparation of SWNTs, since it contains a smaller number of carbon atoms. The bottom portion of the SWNT in Figure 3a shows an amorphous

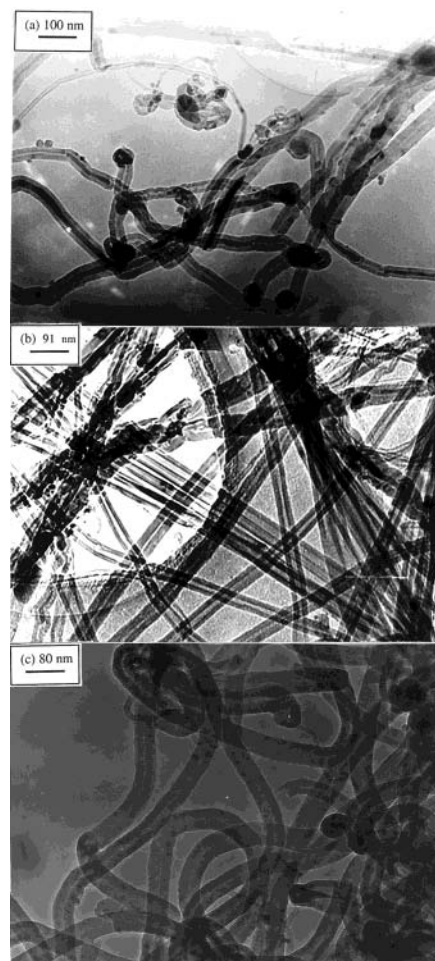


**FIGURE 2.** TEM image of a multiwalled carbon nanotube obtained by pyrolysis of (a) ferrocene at 900 °C in a mixture of 75% Ar/25%  $H_2$  at a flow rate of 900 sccm, (b) a mixture of  $C_2H_2$  (25 sccm) and ferrocene at 1100 °C at 1000 sccm Ar flow, and (c) a mixture of nickelocene and benzene at 900 °C in 85% Ar and 15%  $H_2$  mixture at a flow rate of 1000 sccm.<sup>6,7</sup>

carbon coating around the tube, commonly observed in many of the preparations. This can be avoided by reducing the proportion of the hydrocarbon and mixing hydrogen in the Ar stream. Pyrolysis of cobaltocene and acetylene under similar conditions gives rise to isolated SWNTs. In Figure 3c,d, we show the high-resolution electron microscope (HREM) images of the SWNTs obtained by the pyrolysis of ferrocene with methane at 1100 °C. Surprisingly, the pyrolysis of nickelocene or cobaltocene in admixture with methane under similar conditions did not give SWNTs in good yield. Pyrolysis of binary mixtures (1:1 by weight) of the metalocenes along with acetylene gives good yields of SWNTs, due to the beneficial effect of binary alloys.<sup>12</sup>

SWNTs are obtained in good yields by the pyrolysis of acetylene in mixture with  $Fe(CO)_5$  at 1100 °C employing a setup of the type shown in Figure 1b. We show TEM images of the SWNTs so obtained in Figure 4. Pyrolysis of ferrocene–thiophene mixtures yield SWNTs, but the yield is somewhat low. Pyrolysis of a mixture of benzene and thiophene along with ferrocene (Figure. 1c), however, gives a high yield of SWNTs.<sup>13</sup>

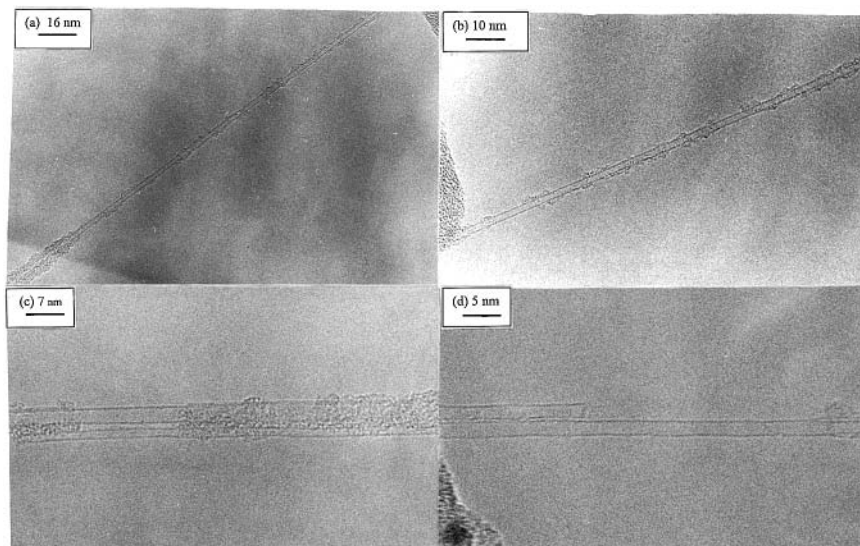


**FIGURE 3.** (a, b) HREM images of SWNTs obtained by the pyrolysis of nickelocene and  $C_2H_2$  at  $1100\text{ }^\circ\text{C}$  in a flow of Ar (1000 sccm) with  $C_2H_2$  flow rate of 50 sccm. (c, d) HREM images of SWNTs obtained by the pyrolysis of ferrocene and  $CH_4$  at  $1100\text{ }^\circ\text{C}$  in a flow of Ar (990 sccm) with  $CH_4$  flow rate of 10 sccm.<sup>11</sup>

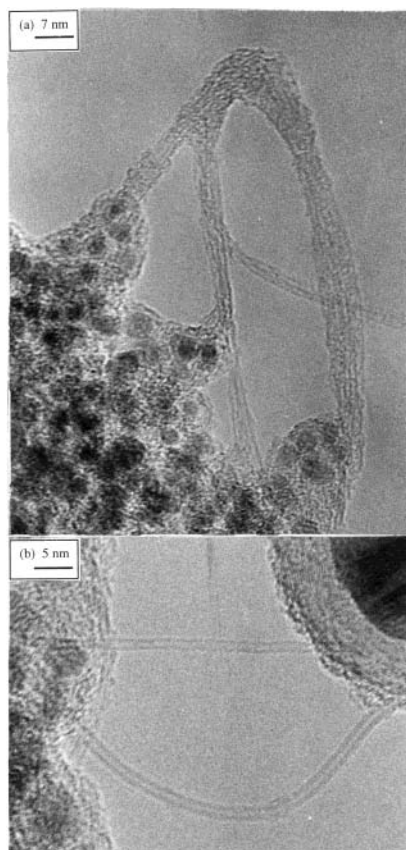


**FIGURE 4.** (a, b) TEM images of SWNTs obtained by the pyrolysis of  $Fe(CO)_5$  and  $C_2H_2$  (flow rate = 50 sccm) at  $1100\text{ }^\circ\text{C}$  in Ar (flow rate = 1000 sccm) flow.<sup>10,11</sup>

TEM examination of the various carbonaceous products obtained from the pyrolysis of hydrocarbons and organometallic precursors indicates that the size of the catalyst particle plays an important role with regard to the nature of the product. In the case of organometallic precursors, it seems that metal nanoclusters of  $\sim 1\text{ nm}$

diameter are produced under controlled conditions. When the concentration of the organometallic precursor is high, MWNTs are formed around the metal particles of 5–20 nm diameter. This is true of carbon nanotubes obtained by the metallocene route.<sup>6,7</sup> In the higher size range of  $\geq 50\text{ nm}$ , graphite-covered metal particles are formed predominantly.<sup>15</sup>

### Aligned Carbon Nanotube Bundles

Since the pyrolysis of mixtures of organometallic precursors and hydrocarbons yields good quantities of multi-walled nanotubes,<sup>6,7</sup> we considered the possibility of obtaining aligned nanotube bundles under appropriate conditions. For this purpose, we carried out pyrolysis of metallocenes along with other hydrocarbon sources, in the apparatus shown in Figure 1a.<sup>10,15,16</sup> To obtain aligned nanotube bundles, a typical heating rate  $50\text{ }^\circ\text{C}/\text{min}$  of the first furnace and an Ar flow rate of 1000 sccm have been employed. Compact aligned nanotube bundles could be obtained by introducing  $C_2H_2$  (50–100 sccm) during the sublimation of ferrocene. Scanning electron microscope images of aligned nanotubes obtained by the pyrolysis of ferrocene are shown in Figure 5. The image in Figure 5a shows the top view of the aligned nanotubes, wherein the nanotube tips are seen. The image in Figure 5b shows the side view. Aligned nanotubes obtained by the pyrolysis of ferrocene with different alkanes are shown in the SEM images in Figure 6. The average length of the nanotubes is generally around  $60\text{ }\mu\text{m}$  with methane and acetylene. In the case of methane, the nanotubes are aligned, but the packing density is not high. The nanotube bundles obtained with ferrocene + acetylene mixtures appear to have a packing density greater than that obtained with Fe/silica catalysts.<sup>17</sup> SEM images of large bundles of the aligned nanotubes are shown in Figure 7. A small proportion of graphite-covered metal nanoparticles is often present along with the nanotubes. In Table 1, we sum-

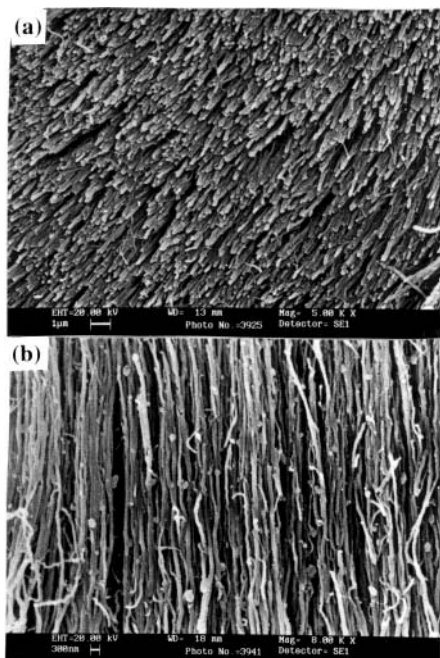


**FIGURE 5.** SEM images of aligned carbon nanotubes obtained by the pyrolysis of ferrocene. (a) and (b) show views of the aligned nanotubes along and perpendicular to the axis of the nanotubes, respectively.<sup>16</sup>

marize the products obtained by the pyrolysis of hydrocarbon + organometallic mixtures at 1100 °C in a stream of Ar + H<sub>2</sub>.

Andrews et al.<sup>18</sup> have carried out the pyrolysis of ferrocene–xylene mixtures to obtain aligned carbon nanotubes. Pyrolysis of Fe(II) phthalocyanine also yields aligned nanotubes.<sup>19</sup> Chen et al.<sup>20</sup> have grown three-dimensional micropatterns of well-aligned carbon nanotubes on photolithographically prepatterned substrates, by the pyrolysis of iron(II) phthalocyanine in an Ar/H<sub>2</sub> atmosphere around 950 °C. They achieved the photopatterning by photolithographic cross-linking of a chemically amplified photoresist layer spin-cast on a quartz plate or a silicon wafer coupled with solution development. Owing to the appropriate surface characteristics, the patterned photoresist layer supports aligned nanotube growth. The difference in the chemical nature between the surfaces covered and uncovered by the photoresist film causes a region-specific growth of nanotubes with different tubular lengths and packing densities leading to the formation of three-dimensional aligned nanotube patterns.

Considering all aspects, we feel that the pyrolysis of organometallic precursors is the most convenient means of preparing aligned MWNTs. The other methods reported

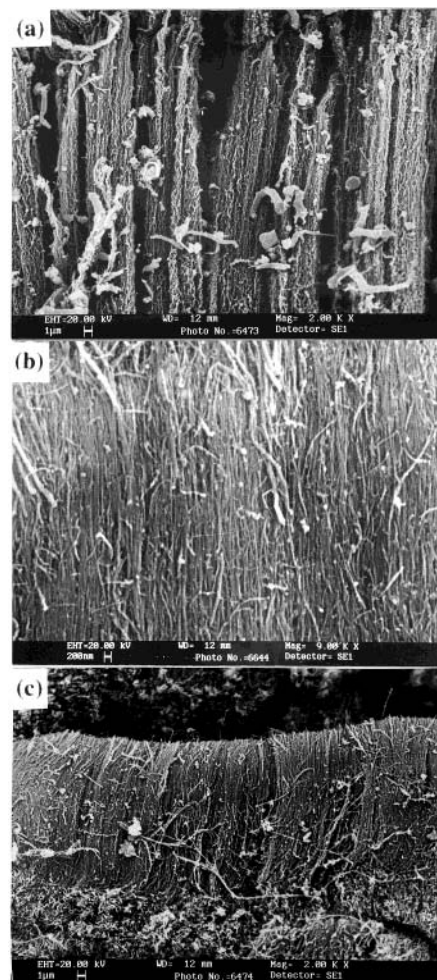


**FIGURE 6.** SEM images showing the bundles of aligned nanotubes obtained by the pyrolysis of ferrocene along with (a) methane, (b) acetylene, and (c) butane (hydrocarbon at 50 sccm) at 1100 °C in a Ar flow of 950 sccm.<sup>15</sup>

in the literature, such as hydrocarbon pyrolysis on patterned metal films,<sup>21</sup> are more difficult and are not amenable for large-scale synthesis. The advantage of the precursor method is that the aligned bundles are produced in one step, at a relatively low cost, without prior preparation of substrates. It is possible that the self-assembly of carbon nanotubes from precursor pyrolysis is influenced by the transition metal particles which take part in the nucleation and growth of the nanotubes. The metal often gets encapsulated to form nanorods or nanoparticles inside the carbon nanotubes. Ferromagnetism of these metal particles is also a property of significance. The iron nanorods encapsulated in the nanotubes exhibit a complex behavior with respect to magnetization reversal and could be useful as probes in magnetic force micros-

**Table 1. Products Obtained by the Pyrolysis of Hydrocarbon–Organometallic Mixtures at 1100 °C**

organometallic precursor	hydrocarbon	inlet	outlet
ferrocene	acetylene	aligned MWNTs, nanorods	metal nanoparticles*
nickelocene	acetylene	MWNTs	SWNTs
cobaltocene	acetylene	MWNTs	SWNTs
ferrocene + nickelocene	acetylene	aligned MWNTs	SWNTs
ferrocene + cobaltocene	acetylene	aligned MWNTs	SWNTs
nickelocene + cobaltocene	acetylene	MWNTs	SWNTs
Fe(CO) <sub>5</sub>	acetylene	MWNTs	SWNTs (bundles)

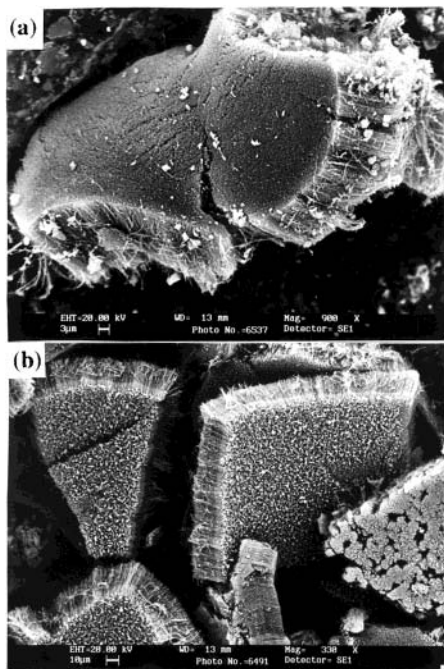


**FIGURE 7.** SEM images showing the bundles of aligned nanotubes obtained by pyrolyzing ferrocene along with (a) acetylene and (b) butane.<sup>15</sup>

copy. Aligned carbon nanotubes are potential candidates for use as field emitters,<sup>14</sup> and the easy synthesis from organometallic precursors is therefore of importance.

## Y-Junction Carbon Nanotubes

Device miniaturization in semiconductor technology is expected to reach its limits due to the inherent quantum effects as one goes toward smaller size. In such a scenario, an alternative would be nanoelectronics based on molecules. The possible use of carbon nanotubes in nanoelectronics has aroused considerable interest. For such applications it is important to be able to connect the nanotubes of different diameters and chirality.<sup>22–24</sup> Complex three-point nanotube junctions have been proposed as the building blocks of nanoelectronics, and in this regard Y- and T-junctions have been considered as prototypes.<sup>25,26</sup> While we would expect an equal number of five- and seven-membered rings to create nanotube junctions, it appears that they can be created with an equal number of five- and eight-membered rings as well.<sup>26</sup> To date, there have been no practical devices made of real three-point nanotube junctions. However, junctions consisting of crossed nanotubes have been fabricated to study their transport characteristics.<sup>27</sup> Y-junction nanotubes have been produced by using Y-shaped nanochannel alumina as templates.<sup>28</sup> We have prepared Y-junction nanotubes in large quantities by carrying out the pyrolysis of a mixture of a metallocene with thiophene.<sup>29,30</sup>

The experimental setup employed by us for the synthesis of the Y-junction nanotubes employed a two-stage furnace system similar to that described earlier<sup>29</sup> (Figure 1c). A known quantity of metallocene was sublimed in the first furnace and carried along with a flow of argon (Ar)

gas to the pyrolysis zone in the second furnace. Simultaneously hydrogen was bubbled through thiophene and was mixed with the argon–metallocene vapors at the inlet of the furnace and carried to the pyrolysis zone. Pyrolyzing the mixed vapors at 1000 °C yielded Y-junction nanotubes in plenty. Pyrolysis of Ni/Fe phthalocyanine in mixture with thiophene was carried out in a similar manner taking phthalocyanine in place of the metallocenes to obtain good Y-junction nanotubes. Pyrolysis of various organometallics with sulfur-containing compounds has shown that pyrolysis of thiophene with nickelocene, ferrocene, and cobaltocene yields excellent Y-junction nanotubes. A TEM image of a Y-junction nanotube obtained by the pyrolysis of nickelocene/thiophene mixture is shown in Figure 8a. A TEM image revealing the presence of several Y-junction carbon nanotubes is shown in Figure 8b. Many of the nanotubes show multiple Y-junctions.

Pyrolysis of thiophene with Fe or Ni phthalocyanine or iron pentacarbonyl also yields Y-junction nanotubes. In Figure 9a, we show few Y-junctions, where as in Figure 9b we show the multiple junctions formed continuously by the pyrolysis of thiophene with Ni phthalocyanine. While the pyrolysis of nickelocene with CS<sub>2</sub> yields similar junctions, the yield and quality of the nanotubes is not satisfactory. At higher flow rates of CS<sub>2</sub>, with ferrocene it pyrolyses and gives Y-junction carbon fibers. In Figure 9c we show the Y-junctions obtained by the pyrolysis of thiophene with Fe phthalocyanine. Pyrolysis of thiophene with Fe(CO)<sub>5</sub> carried out by bubbling H<sub>2</sub> (50–100 sccm) through the pentacarbonyl along with Ar (150–200 sccm) bubbled through thiophene showed the presence of interesting junction structures as revealed in Figure 9d. The pyrolysis of thiophene over a Ni(Fe)/SiO<sub>2</sub> catalyst provides an alternative procedure to the metallocene route, but the yield of Y-junction tubes is rather low. The availability of large quantities of Y-junctions should render them useful for exploitation in nanoelectronics. Compositional analysis at the Y-junction has shown absence of sulfur indicating that the junction is formed by the curvature caused by different carbon rings. The metal nanoparticles abstract the sulfur from thiophene forming a sulfide, the remaining carbon fragment probably being involved in ring formation.

HREM images show that the graphitic layers bend parallelly with respect to the junction in many of these nanotubes. Our studies in collaboration with Torsteen Seeger and Manfred Ruhle have shown that the Y-junction tubes are entirely composed of carbon with no sulfur impurity. These observations suggest the presence of equal numbers of five- and seven-/eight-membered rings at the junctions. The metal particles formed in the pyrolysis contain both sulfur and carbon.

Scanning tunneling spectroscopic studies of Y-junction carbon nanotubes show interesting diodelike device characteristics at the junctions. A typical *I*–*V* curve obtained from positioning the tip atop a Y-junction (the point of contact between the three arms) as well as on the individual arms of the Y-junction is shown in Figure 10. The *I*–*V* plot at the junction is asymmetric (Figure 10b)

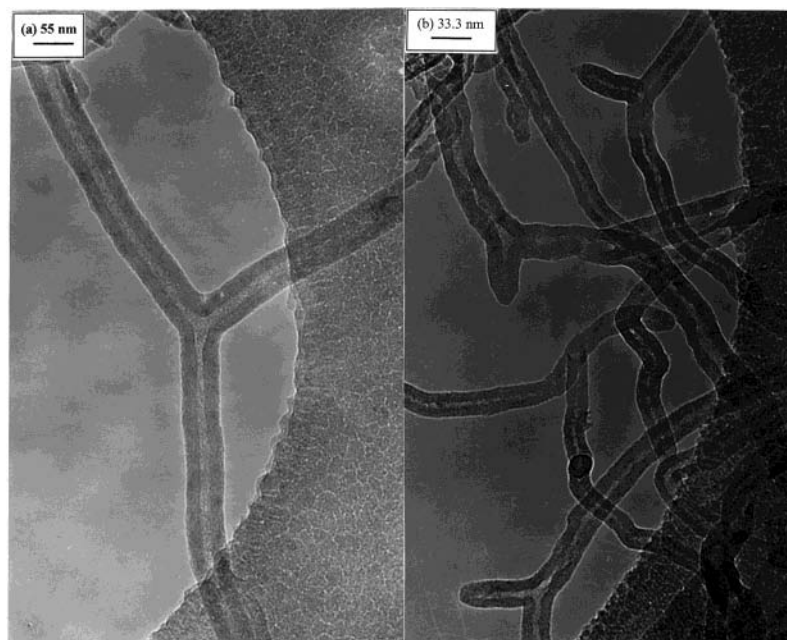


FIGURE 8. (a, b) TEM images of Y-junction carbon nanotubes obtained by the pyrolysis of nickelocene and thiophene at 1000 °C.<sup>29</sup>

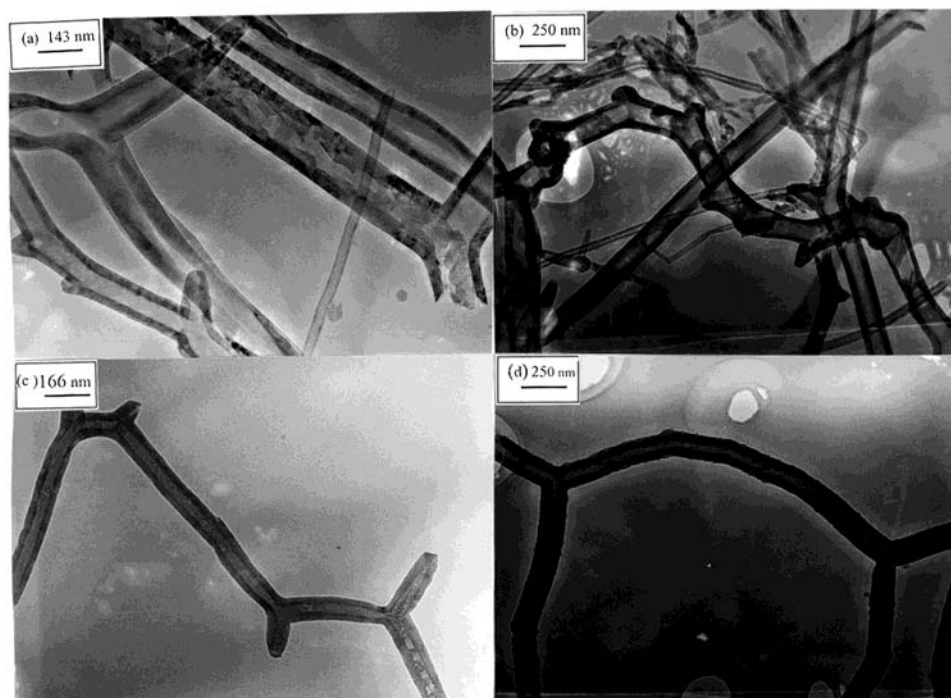


FIGURE 9. TEM images of Y-junction nanotubes: (a, b) obtained by the pyrolysis of thiophene along with Ni phthalocyanine at 1000 °C; (c) obtained by the pyrolysis of thiophene along with Fe phthalocyanine at 1000 °C; (d) obtained by the pyrolysis of an  $\text{Fe}(\text{CO})_5$ –thiophene mixture at 1000 °C.<sup>30</sup>

with respect to bias polarity, unlike that along the arm (Figure 10a). The insets in Figure 10 gives a plot of differential conductance vs bias with respect to zero bias which is symmetric in Figure 10a and asymmetric in Figure 10b. Such asymmetry is characteristic of a junction diode, and this in turn indicates the existence of intramolecular junctions in the carbon nanotubes. The findings discussed above open up the possibility of assembling carbon nanotubes possessing novel devicelike properties<sup>29,31–33</sup> into multifunctional circuits and ultimately toward the realization of a carbon nanotube based

computer chip. Rueckes et al.<sup>34</sup> have described the concept of carbon-nanotube-based nonvolatile random access memory for molecular computing. The viability of the concept has been demonstrated.

### Nanorods, Nanowires, and Nanotubes of Other Materials

Preparation of metal nanorods covered by carbon has been reported in the recent literature.<sup>10,35–37</sup> The organometallic precursor route provides a means of preparing

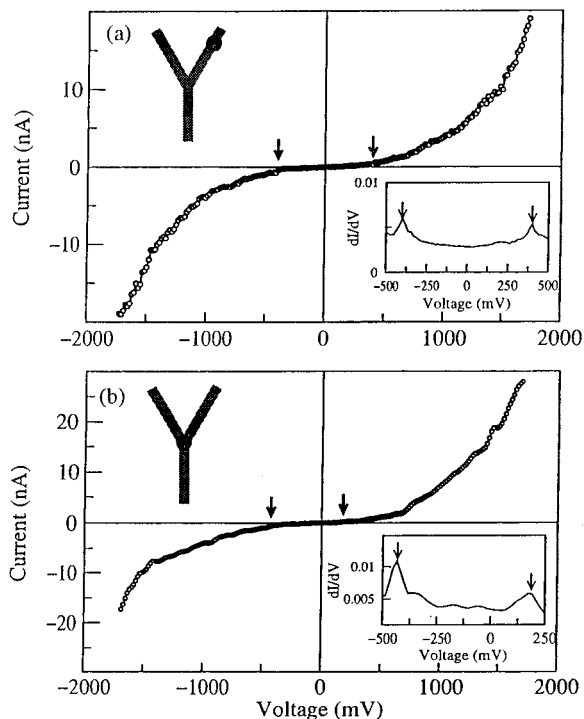


**FIGURE 10.**  $I$ - $V$  curves collected from different points in a Y-junction carbon nanotube (a) from one of the arms away from the junction and (b) from the junction of the three arms. Inset show plots of  $dI/dV$  vs bias voltage. The observed gaps are indicated by arrows.<sup>29</sup>

metal nanorods. The pyrolysis of ferrocene + hydrocarbon mixtures or of ferrocene alone yields iron nanorods encapsulated inside the carbon nanotubes as evidenced from TEM, the proportion of the nanorods depending on the proportion of ferrocene. Typical TEM images of such nanorods are shown in Figure 11a,b. The selected area electron diffraction (SAED) pattern of the nanorods (inset in Figure 11c) shows spots due to (010) and (011) planes of  $\alpha$ -Fe. The HREM image of the iron nanorod in Figure 11c shows well-resolved (011) planes of  $\alpha$ -Fe in single-crystalline form. X-ray diffraction patterns show the presence of  $\alpha$ -Fe with a small portion of  $\text{Fe}_3\text{C}$  as the minor phase. In addition to the nanorods, iron nanoparticles (20–40 nm diameter) encapsulated inside the graphite layers are also obtained in many of the preparations. The iron nanorods and nanoparticles are well protected against oxidation by the graphitic layers. Ni/Fe phthalocyanines can be used in the place of metallocenes to prepare metal nanowires. However, the yields are not as good as in the case of metallocenes.

There are several reports on the preparation of SiC nanowires in the literature but fewer on the preparation of  $\text{Si}_3\text{N}_4$  nanowires.<sup>38,39</sup> The methods employed for the synthesis of SiC nanowires have been varied. Since both SiC and  $\text{Si}_3\text{N}_4$  are products of the carbothermal reduction of  $\text{SiO}_2$ , it should be possible to establish conditions wherein one set of specific conditions favor one over the other. We have been able to prepare  $\text{Si}_3\text{N}_4$  nanowires,<sup>40</sup> by reacting multiwalled carbon nanotubes produced by ferrocene pyrolysis with ammonia and silica gel at 1360

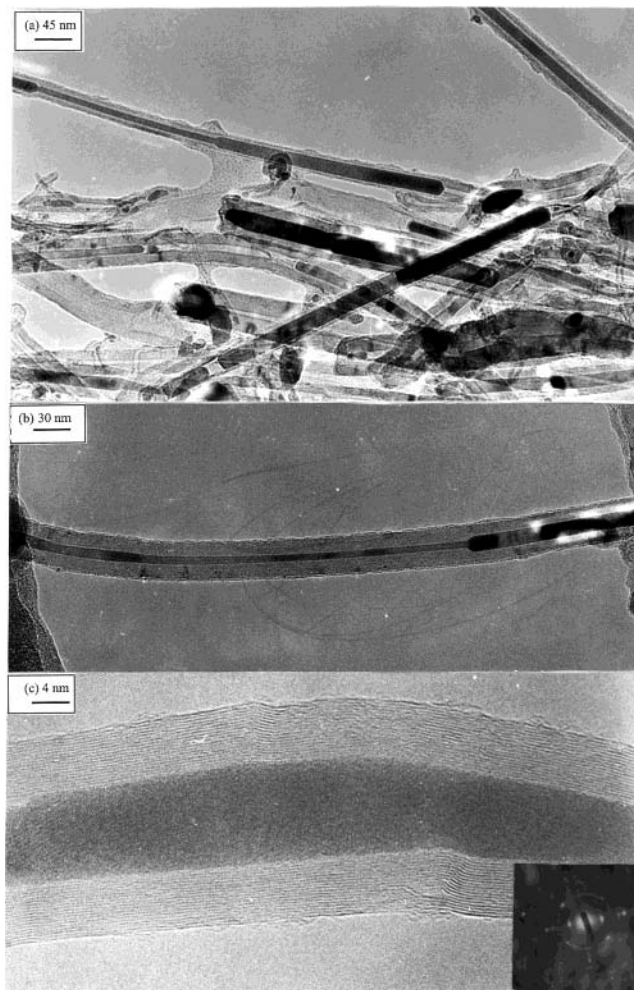


**FIGURE 11.** (a, b) TEM images of the iron nanorods encapsulated inside the carbon nanotubes from aligned nanotube bundles. (c) HREM image of a single-crystal iron nanorod encapsulated inside a carbon nanotube. The inset in (c) represents the selected area electron diffraction (SAED) pattern of a iron nanorod.<sup>16,35</sup>

°C. The MWNTs were used as a carbon source in the carbothermal reduction because they have higher thermal stability compared to activated carbon. The reaction of MWNTs with silica gel and  $\text{NH}_3$  at 1360 °C yields a mixture of  $\alpha$ - and  $\beta$ - $\text{Si}_3\text{N}_4$ . SEM images of the product obtained by this reaction showed the nanowires to have large diameters (5–7  $\mu\text{m}$ ), with lengths of the order of hundreds of micrometers (Figure 12a). By addition of catalytic iron particles (0.5 at. %), we obtain  $\beta$ -SiC nanowires under the same conditions<sup>40</sup> (Figure 12b).

Several chemical methods of preparing boron nitride nanotubes and nanowires have been investigated.<sup>41</sup> The general methods involve reacting boric acid with ammonia in the presence of MWNTs. Good yields of clean BN nanotubes are obtained with MWNTs. Aligned BN nanotubes are obtained by heating aligned bundles of MWNTs with boric acid in the presence of ammonia at the 1000°–1300 °C range. The SEM images of aligned BN nanotube bundles shown in Figure 13 a,b clearly reveal BN nanotubes aligned in two different orientations. The carbon MWNTs appear to not only take part in the reaction but also serve as templates. The average outer diameter of the

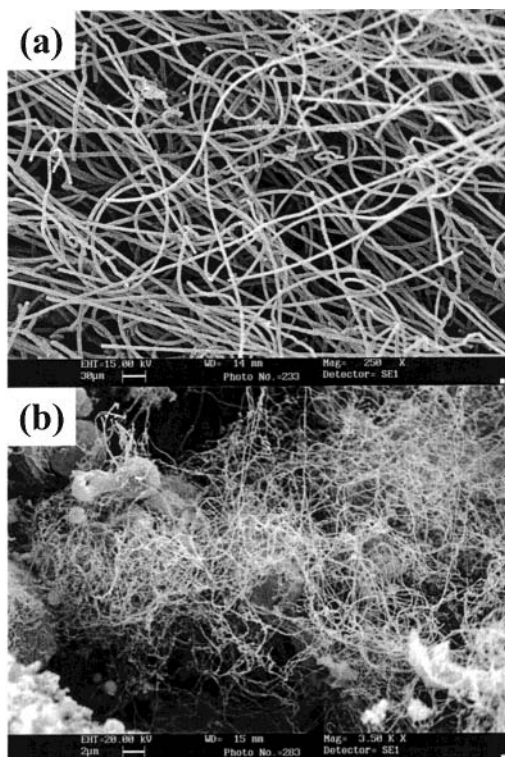


**FIGURE 12.** (a) SEM image of  $\text{Si}_3\text{N}_4$  nanowires obtained by the reaction of aligned multiwalled nanotubes (produced by metallocene route) with silica gel at  $1360^\circ\text{C}$ . (b) SiC nanowires.<sup>40</sup>

aligned BN nanotubes varies from 15 to 40 nm as revealed by the TEM image in Figure 13c. This suggests that, during the formation of BN nanotubes, the carbon MWNTs not only take part in the reaction but also serve as templates. It is noteworthy that the BN nanotubes can be produced at a temperature as low as  $1000^\circ\text{C}$  by this procedure. On the basis of elemental analysis and X-ray diffraction, it is found that the carbon content of the BN nanotubes becomes marginal if the initial proportion of carbon nanotubes is kept low.

Gallium nitride nanowires have been prepared by us by employing several procedures involving the use of carbon nanotube templates.<sup>42</sup> We have employed gallium acetylacetonate as the precursor for the in-situ production of small particles of the oxide ( $\text{GaO}_x$ ) which then react with  $\text{NH}_3$  vapor around  $900^\circ\text{C}$  in the presence of nanotubes. When multiwalled carbon nanotubes prepared by arc discharge are used as templates, the yield of the GaN nanowires is excellent and the diameter of the majority of the nanowires is in the 35–100 nm range. The length of the nanowires extends to a few micrometers. The linear nanowires are generally single crystalline, showing a layer spacing of 0.276 nm corresponding to the [100] planes. This variation in the diameter of the nanowires occurs because of the nonuniformity in the diameter of the nanotubes. The diameter of the nanowires could be reduced to 20 nm by using single-walled nanotubes in place of multiwalled nanotubes. The growth direction of the nanowires is nearly perpendicular to the [100] planes. The nanowires show satisfactory photoluminescence characteristics similar to those of bulk GaN. The non-carbon

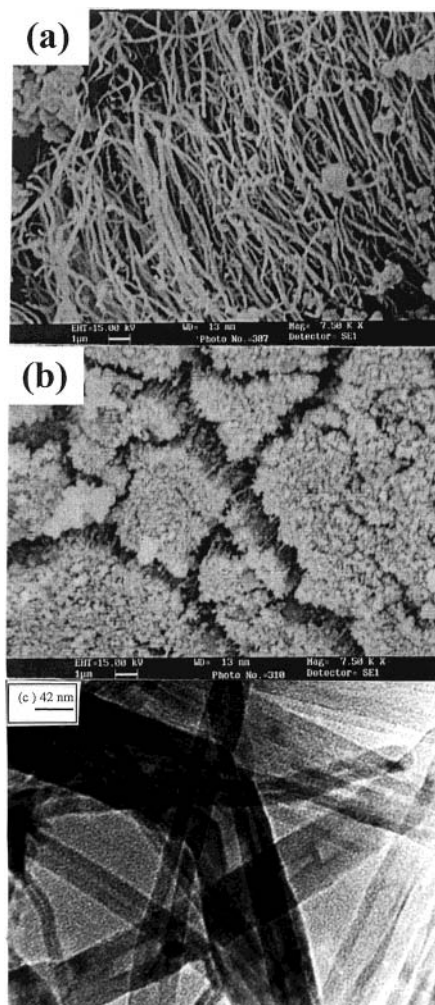


**FIGURE 13.** (a, b) SEM images of BN nanotubes obtained by heating aligned bundles of MWNTs with boric acid in the presence of ammonia at  $1300^\circ\text{C}$ . (c) TEM image of the BN nanotubes obtained by the same procedure as in (a) and (b).<sup>41</sup>

nanowires and nanotubes have potential applications. For example, GaN nanowires, suitably doped, can have uses in nanoelectronics and in optical devices. BN nanotubes and  $\text{Si}_3\text{N}_4$  nanowires are useful ceramic materials.

## Properties

Field emission properties of carbon nanotubes have direct applications in vacuum microelectronic devices.<sup>43–46</sup> We have found that carbon nanotubes produced by the pyrolysis of ferrocene on a pointed tungsten tip exhibit high emission current densities with good performance characteristics.<sup>47</sup> In Figure 14a we show a typical  $I-V$  plot for the carbon nanotube covered tungsten tip for currents ranging from 0.1 nA to 1 mA. The applied voltage was 4.3 kV for a total current of  $1\ \mu\text{A}$  and 16.5 kV for  $1000\ \mu\text{A}$ . The Fowler–Nordheim (F–N) plot shown in Figure 14b has two distinct regions. The behavior is metal-like in the low-field region, while it saturates at higher fields as the voltage is increased. We have obtained a field emission current density of  $1.5\ \text{A cm}^{-2}$  at a field of 290 V/mm, a value considerably higher than that found with planar cathodes.



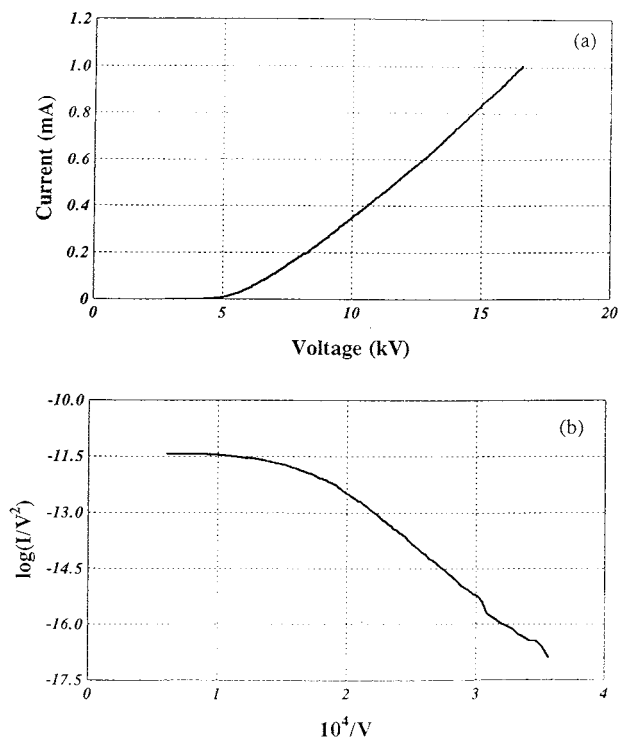


FIGURE 14.  $I$ - $V$  characteristics showing field emission currents in the range of 0.1 nA to 1 mA. (b) Fowler-Nordheim plot corresponding to the data in (a).<sup>47</sup>

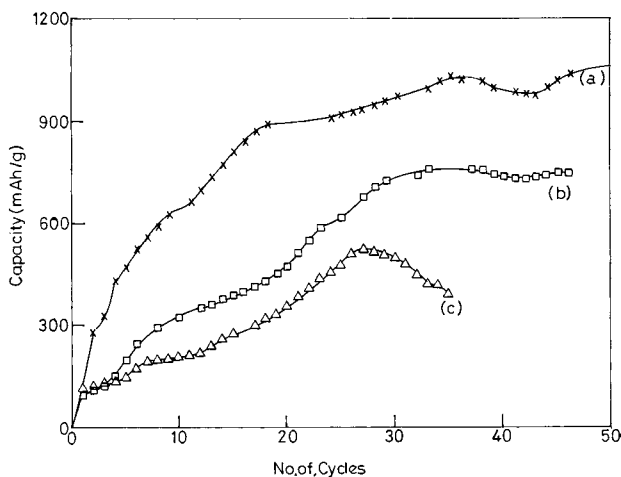


FIGURE 15. Comparison of electrochemical charging capacity of hydrogen of (a) aligned MWNT bundles, (b) SWNTs, and (c) MWNTs (arc-generated).<sup>49</sup>

Accordingly, the field enhancement factor calculated from the slope of the F-N plot in the low-field region is also large. The field emission micrographs reveal the lobe structure symmetries typical of carbon nanotube bundles. The emission current is remarkably stable over an operating period of more than 3 h for various current values in the 10–500 mA range. The relative fluctuations decrease with increasing current level, and the emitter can be operated continuously at the high current levels for at least 3 h without any degradation in the current. It appears that aligned carbon nanotubes from ferrocene pyrolysis hold promise as good field electron emission sources.

Carbon nanotubes are considered to be good hosts for hydrogen storage, although there is some controversy about the magnitude of the hydrogen uptake.<sup>35,48</sup> High-pressure adsorption experiments carried out by us with G. Gundiah show that the storage capacity of compact aligned nanotubes prepared by the pyrolysis of ferrocene-hydrocarbon mixtures is between 3 and 4 wt % (143 bar, 27 °C). Electrochemical hydrogen storage in these nanotubes is also substantial. In Figure 15 a–c we show (for comparison) the plots of electrochemical charging capacity of aligned nanotubes, SWNTs, and MWNTs (arc-generated), respectively.<sup>49</sup> Electrodes made out of aligned MWNTs clearly demonstrate higher electrochemical charging capacities up to 1100 mA h g<sup>-1</sup> which correspond to a hydrogen storage capacity of 3.75 wt %. SWNTs and MWNTs (arc-generated), however, show capacity in the range of 2–3 wt %.

## Concluding Remarks

Although arc evaporation of graphite has traditionally been found to yield both single-walled and multiwalled carbon nanotubes, the pyrolysis of organometallic precursors with or without the presence of additional carbon sources seems to provide a direct and effective method of producing nanotubes of various kinds. A particularly important finding is the one-step synthesis of aligned carbon nanotubes and Y-junction nanotubes which cannot be made by arc evaporation or other methods easily. It is also noteworthy that nanotubes produced by organometallic precursors may also find applications in field emission and hydrogen storage. The successful synthesis of nanowires of gallium nitride and silicon nitride and of boron nitride nanotubes by using carbon nanotubes produced from organometallic precursors is also of interest.

The authors thank the Department of Science and Technology, Government of India, and the DRDO (India) for supporting this research. They acknowledge productive collaboration with Dr. B. C. Satishkumar, Dr. R. Sen, Mr. F. L. Deepak, and Mr. G. Gundiah.

## References

- (1) Iijima, S. Helical microtubules of graphitic carbon. *Nature* **1991**, *354*, 56.
- (2) Jose-Yacamán, M.; Miki-Yoshida, M.; Rendon, L.; Santiesteban, T. G. Catalytic growth of carbon microtubules with fullerene structure. *Appl. Phys. Lett.* **1993**, *62*, 202.
- (3) Ivanov, V.; Nagy, J. B.; Lambin, Ph.; Lucas, A.; Zhang, X. B.; Zhang, X. F.; Bernaerts, D.; Van Tendeloo, G.; Amelinckx, S.; Van Landuyt, J. The study of carbon nanotubules produced by catalytic method. *Chem. Phys. Lett.* **1994**, *223*, 329.
- (4) Hernadi, K.; Fonseca, A.; Nagy, J. B.; Bernaerts, D.; Riga, J.; Lucas, A. Catalytic synthesis and purification of carbon nanotubes. *Synth. Met.* **1996**, *77*, 31.
- (5) Rodriguez, N. M. A review of catalytically grown carbon nanofibers. *J. Mater. Res.* **1993**, *8*, 3233.
- (6) Sen, R.; Govindaraj, A.; Rao, C. N. R. Carbon nanotubes by metallocene route. *Chem. Phys. Lett.* **1997**, *267*, 276.
- (7) Sen, R.; Govindaraj, A.; Rao, C. N. R. Metal-filled and hollow carbon nanotubes obtained by the decomposition of metal containing free precursor molecules. *Chem. Mater.* **1997**, *9*, 2078.
- (8) Yudasaka, M.; Kikuchi, R.; Ohki, Y.; Yoshimura, S. Nitrogen-containing carbon nanotube growth from Ni-phthalocyanine by chemical vapor deposition. *Carbon* **1997**, *35*, 195.
- (9) Fan, S.; Chapline, M. C.; Franklin, N. R.; Tomblor, T. W.; Cassel, A. M.; Dai, H. Self-oriented regular arrays of carbon nanotubes and their field emission devices. *Science* **1999**, *283*, 512.

- (10) Rao, C. N. R.; Govindaraj, A.; Sen, R.; Satishkumar, B. C. Synthesis of multiwalled and single-walled nanotubes, aligned bundles and nanorods by employing organometallic precursors. *Mater. Res. Innovations* **1998**, *2*, 128.
- (11) Satishkumar, B. C.; Govindaraj, A.; Sen, R.; Rao, C. N. R. Single-walled nanotubes by the pyrolysis of acetylene-organometallic precursors. *Chem. Phys. Lett.* **1998**, *293*, 47.
- (12) Seraphin, S.; Zhou, D. Single-walled carbon nanotubes produced at high yield by mixed catalysts. *Appl. Phys. Lett.* **1994**, *64*, 2087.
- (13) Cheng, H. M.; Li, F.; Su, G.; Pan, H. Y.; He, L. L.; Sun, X.; Dresselhaus, M. S. Large-scale and low-cost synthesis of single-walled carbon nanotubes by the catalytic pyrolysis of hydrocarbons. *Appl. Phys. Lett.* **1998**, *72*, 3282.
- (14) de Heer, W. A.; Bonard, J. M.; Fauth, K.; Chatelain, A.; Forro, L.; Ugarte, D. Electron field emitters based on carbon nanotube films. *Adv. Mater.* **1997**, *9*, 87.
- (15) Satishkumar, B. C.; Govindaraj, A.; Rao, C. N. R. Bundles of aligned carbon nanotubes obtained by the pyrolysis of ferrocene-hydrocarbon mixtures: role of the metal nanoparticles produced in situ. *Chem. Phys. Lett.* **1999**, *307*, 158.
- (16) Rao, C. N. R.; Sen, R.; Satishkumar, B. C.; Govindaraj, A. Aligned nanotube bundles from ferrocene pyrolysis. *Chem. Commun.* **1998**, 1525.
- (17) Pan, Z. W.; Xie, S. S.; Chang, B. H.; Sun, L. F.; Zhou, W. Y.; Wang, G. Direct growth of aligned open carbon nanotubes by chemical vapor deposition. *Chem. Phys. Lett.* **1999**, *299*, 97.
- (18) Andrews, R.; Jacques, D.; Rao, A. M.; Derbyshire, F.; Qian, D.; Fan, X.; Dickey, E. C.; Chen, J. Continuous production of aligned carbon nanotubes: a step closer to commercial realization. *Chem. Phys. Lett.* **1999**, *303*, 467.
- (19) Huang, S.; Mau, A. W. H.; Turney, T. W.; White, P. A.; Dai, L. Patterned growth of well-aligned carbon nanotubes: A soft-lithographic approach. *J. Phys. Chem. B* **2000**, *104*, 2193.
- (20) Chen, Q.; Dai, L. Three-dimensional micropatterns of well-aligned carbon nanotubes produced by photolithography. *J. Nanosci. Nanotechnol.* **2001**, *1*, 43.
- (21) Terrones, M.; Grobert, N.; Zhang, J. P.; Terrones, H.; Olivares, J.; Hsu, H. K.; Hare, J. P.; Cheetham, A. K.; Kroto, H. W.; Walton, D. R. M. Preparation of aligned carbon nanotubes catalysed by laser-etched cobalt thin films. *Chem. Phys. Lett.* **1998**, *285*, 299.
- (22) Chico, L.; Crespi, V. H.; Benedict, L. X.; Louie, S. G.; Cohen, M. L. Pure carbon nanoscale devices: Nanotube heterojunctions. *Phys. Rev. Lett.* **1996**, *76*, 971.
- (23) Kouwenhoven, L. Single-molecule transistors. *Science* **1997**, *275*, 1896.
- (24) McEuen, P. L. Nanotechnology: Carbon-based electronics. *Nature (London)* **1998**, *393*, 15.
- (25) Menon, M.; Srivastava, D. Carbon nanotube "T-junctions": Nanoscale metal-semiconductor-metal contact devices. *Phys. Rev. Lett.* **1997**, *79*, 4453.
- (26) Menon, M.; Srivastava, D. Carbon nanotube based molecular electronic devices. *J. Mater. Res.* **1998**, *13*, 2357.
- (27) Fuhrer, M. S.; Nygard, J.; Shih, L.; Forero, M.; Yoon, Y. G.; Mazzone, M. S. C.; Choi, H. J.; Ihm, J.; Louie, S. G.; Zettl, A.; McEuen, P. L. Crossed nanotube junctions. *Science* **2000**, *288*, 494.
- (28) Li, J.; Papadopoulos, C.; Xu, J. Nanoelectronics: Growing Y-junction carbon nanotubes. *Nature (London)* **1999**, *402*, 253.
- (29) Satishkumar, B. C.; Thomas, P. J.; Govindaraj, A.; Rao, C. N. R. Y-junction carbon nanotubes. *Appl. Phys. Lett.* **2000**, *77*, 2530.
- (30) Deepak, F. L.; Govindaraj, A.; Rao, C. N. R. Synthetic strategies for Y-junction carbon nanotubes. *Chem. Phys. Lett.* **2001**, *345*, 5.
- (31) Tans, S. J.; Verschueren, A. R. M.; Dekker, C. Room-temperature transistor based on a single carbon nanotube. *Nature* **1998**, *393*, 49.
- (32) Martel, R.; Schmidt, T.; Shea, H. R.; Hertel, T.; Avouris, Ph. Single- and multiwall carbon nanotube field-effect transistors. *Appl. Phys. Lett.* **1998**, *73*, 2447.
- (33) Yao, Z.; Postma, H. W. Ch.; Balents, L.; Dekker, C. Carbon nanotube intramolecular junctions. *Nature* **1999**, *402*, 273.
- (34) Rueckes, T.; Kim, K.; Joseluich, E.; Tsang, G. Y.; Cheung, C. L.; Leiber, C. M. Carbon nanotube-based nonvolatile random access memory for molecular computing. *Science* **2000**, *289*, 94.
- (35) Rao, C. N. R.; Satishkumar, B. C.; Govindaraj, A.; Nath, M. Nanotubes. *Chem. Phys. Chem.* **2001**, *2*, 78.
- (36) Morales, A. M.; Leiber, C. M. A laser ablation method for the synthesis of crystalline semiconductor nanowires. *Science* **1998**, *279*, 208.
- (37) Zhang, Y.; Suenaga, K.; Colliex, C.; Iijima, S. Coaxial nanocable: Silicon carbide and silicon oxide sheathed with boron nitride and carbon. *Science* **1998**, *281*, 973.
- (38) Han, W.; Fan, S.; Li, Q.; Gu, B.; Zhang, X.; Yu, D. Synthesis of silicon nitride nanorods using carbon nanotube as a template. *Appl. Phys. Lett.* **1997**, *71*, 2271.
- (39) Wang, M. J.; Wada, H. Synthesis and characterization of silicon nitride whiskers. *J. Mater. Sci.* **1990**, *25*, 1690. Wu, X. C.; Song, W. H.; Zhao, B.; Huang, W. D.; Pu, M. H.; Sun, Y. P.; Du, J. J. Synthesis of coaxial nanowires of silicon nitride sheathed with silicon and silicon oxide. *Solid State Commun.* **2000**, *115*, 683.
- (40) Gundiah, G.; Madhav, G. V.; Govindaraj, A.; Rao, C. N. R. Synthesis and characterization of silicon carbide, silicon oxynitride and silicon nitride nanowires. *J. Mater. Chem.* **2002**, *12*, 1606-1611.
- (41) Deepak, F. L.; Mukhopadhyay, K.; Vinod, C. P.; Govindaraj, A.; Rao, C. N. R. Boron nitride nanotubes and nanowires. *Chem. Phys. Lett.* **2002**, *353*, 345.
- (42) Deepak, F. L.; Govindaraj, A.; Rao, C. N. R. Single-crystal GaN nanowires. *J. Nanosci. Nanotechnol.* **2001**, *1*, 303.
- (43) de Heer, W. A.; Chatelain, A.; Ugarte, D. A carbon nanotube field-emission electron source. *Science* **1995**, *270*, 1179.
- (44) Wang, Q. H.; Corrigan, T. D.; Dai, J. Y.; Chang, R. P. H.; Krauss, A. R. Field emission from nanotube bundle emitters at low fields. *Appl. Phys. Lett.* **1997**, *70*, 3308.
- (45) Bonard, J.-M.; Maier, F.; Stockli, T.; Chatelain, A.; de Heer, W. A.; Salvetat, J.-P.; Ferro, L. Field emission properties of multiwalled carbon nanotubes. *Ultramicroscopy* **1998**, *73*, 7.
- (46) Saito, Y.; Hamaguchi, K.; Hata, K.; Tohji, K.; Kasuya, A.; Nishina, Y.; Uchida, K.; Tasaka, Y.; Ikazaki, F.; Yumura, M. Field emission from carbon nanotubes; Purified single-walled and multiwalled tubes. *Ultramicroscopy* **1998**, *73*, 1.
- (47) Sharma, R. B.; Tondare, V. N.; Joag, D. S.; Govindaraj, A.; Rao, C. N. R. Field emission from carbon nanotubes grown on a tungsten tip. *Chem. Phys. Lett.* **2001**, *344*, 283.
- (48) Dresselhaus, M. S.; Williams, K. A.; Eklund, P. C. Hydrogen adsorption in carbon materials. *MRS Bull.* **1999**, *24*, 45.
- (49) Rajalakshmi, N.; Dhathathreyan, K. S.; Govindaraj, A.; Rao, C. N. R. To be submitted for publication.

AR0101584